Journal of Physics: Conference Series **2586** (2023) 012067 doi:10.1088/1742-6596/2586/1/012067

Evolution of fragment production at the onset of Multifragmentation

E Geraci[1,2], G Cardella[2], M Colonna[3], E De Filippo[2], B Gnoffo[1,2], C Maiolino[3], NS Martorana[1,3], A Pagano[2], EV Pagano[3], S Pirrone[2], G Politi[1,2], P Russotto[3], F Rizzo[1,3], A Trifiró[4,2], M Trimarchi[4,2], S Barlini[5], R Bougault[6], G Casini[5], M D'Agostino[7], F Gramegna[8], N Le Neindre[6] and S Piantelli[5]

[1] Dipartimento di Fisica e Astronomia "Ettore Majorana", Università degli Studi di Catania - Catania, Italy
[2] INFN, Sezione di Catania, Catania, Italy
[3] INFN, Laboratori Nazionali del Sud, Catania, Italy
[4] Dipartimento di Scienze MIFT, Università degli Studi di Messina, Messina, Italy
[5] INFN, Sezione di Firenze and Università degli Studi di Firenze, Firenze, Italy
[6] LPC Caen, ENSICAEN, University of Caen, CNRS/IN2P3, Caen, France
[7] INFN, Sezione di Bologna and Università degli Studi di Bologna, Italy
[8] Laboratori Nazionali di Legnaro, INFN, Italy

elena.geraci@ct.infn.it

Abstract. The onset of Multifragmentation phenomenon is investigated at low excitation energies. A detailed study on the origin of Intermediate Mass Fragment (IMF, Z>=3) produced in central collisions in the ^{58}Ni+^{40}Ca reaction at 25 AMeV is presented. The experimental campaign was performed with CHIMERA multi-detector at INFN Laboratori Nazionali del Sud in Catania (Italy). The multiple identification techniques of the 4π apparatus, together with low detection thresholds, enable the performance of a careful selection of Fusion-evaporation residues, Multifragmentation sources and their decay products. Comparisons with dynamical approach based on Boltzmann-Langevin-One-Body (BLOB) model predictions coupled with sequential emission code, were used as useful tools to depict and understand the characteristics of fragments emitted from an equilibrated compound nucleus or formed simultaneously in the multifragmenting source. A comparison with the preliminary results obtained for fragment production in central collisions of the same system, ^{58}Ni+^{40}Ca, at higher incident energies E_{beam}=35AMeV, allows to study and characterize the evolution of multifragmentation phenomenon at the lower end of Fermi energies.

1. Introduction

In the Fermi energies domain, heavy ion collisions reveal a competition between one body dissipation mechanisms, predominant at low energies, and two body dissipation mechanisms, prevailing at relativistic energies. At low incident energies, mean field effects determine the features of reaction mechanisms; in central collisions the formation of a compound nucleus, which evolves to an evaporation residue by means of statistical emissions of light charged particles, gamma rays and some fragments, is

observed. At higher incident energies the nucleon-nucleon interaction triggers the production of fragments and central collisions are characterized by the production of Intermediate Mass Fragments (IMF), which are a peculiar occurrence in the Fermi energy reaction products, identified as Multifragmentation. In a Multifragmentation event, after the pre-equilibrium emissions, a simultaneous formation of fragments is expected, in which the fragments (IMF), with a charge ranging from 3 to 30-40, are emitted isotropically in one step process, occurring in time range around 50-100 fm/c.The process is driven by the dynamics of the collisions and transport properties of nuclear matter. Sequential statistical models are not able to reproduce the observed emission characteristics. On the contrary, in fusion-evaporation events, the excited compound nucleus decays by evaporation of light charged particles (Z<=2) and radiation emission, leaving a massive residual nucleus. Between successive emissions there is enough time for emitting nucleus to reach a new equilibrium state, so that particles are emitted sequentially and without any correlation and the process is dominated by a statistical occupancy of phase space [1].
It is, consequently, very interesting to study the evolution of fragment production at the onset of Multifragmentation, where a competition between sequential secondary decays [2][3], accountable to produce small fragments, and multifragmentation phenomena, giving rise to 2, 3 or more fragments simultaneously, is observed [4][5] [6].

2. ^{58}Ni+^{40}Ca at 25 AMeV

2.1. Experimental Data Detection

The experiment was performed at the INFN Laboratori Nazionali del Sud (LNS), in Catania (Italy), where ^{58}Ni and ^{62}Ni beams were accelerated at 25 AMeV by the Super Conducting Cyclotron on ^{40}Ca and ^{48}Ca targets. The experiment represented the first part of an experimental campaign devoted to the study of central collisions where sources of one hundred nucleons were produced, with excitation energies around 2-4 AMeV. Produced fragments were detected by the CHIMERA 4π multi-detector, consisting of 1192 Silicon-CsI(Tl) telescopes, arranged in 26 rings covering 95% of the total solid angle [7][8].

CHIMERA multidetector is characterized by very low identification thresholds, obtained through the time of flight (TOF) technique, performed using the cyclotron radio frequency and the silicon signals. The TOF technique allows the direct measurement of fragment velocities that combined with energy measurements grants the mass estimation of particles stopped in silicon detectors. This is particularly useful for the identification, in mass and velocity, of the evaporation residues and of the emitted fragments produced at this lower energies' domain.

The atomic number Z of reaction products punching through the silicon detectors was determined by means of the standard ΔE–E identification technique. This technique was used to also obtain the mass of fragments with $3 \leq Z \leq 8$, detected at laboratory polar angles greater than 13 degrees.

Incomplete or incorrectly reconstructed events were excluded restricting our analysis to events where the sum of the charges (Ztot) of all detected fragments was in the range $80\% < Ztot < 105\%$ of sum of projectile and target charges and the total reconstructed longitudinal momentum (Pz) was in the range $80\% < Pz < 105\%$ of the linear momentum of the projectile.

2.2. Central Collisions Selection

Central collisions were selected imposing a cut on the Total Kinetic Energy (TKE), defined as the sum of the kinetic energies of all reaction products with a charge $Z \geq 3$. The evolution of the reaction mechanisms on different ranges of TKE can be found in [9]. In particular, the condition TKE<700 MeV selected events where a massive fragment, characterized by a velocity close to the center of mass velocity, is emitted together with some light charged particles, as can be seen in the left panel of Fig.1. The statistic of this subset amounts to 4% of the total well reconstructed events. The presence of a massive fragment encourages to associate these events to collisions where an Evaporation Residue

emerges in the final states, due to predominance of a one-body dissipation mechanism. In order to inspect the existence of fragments coming from a multifragmenting source, a further selection was performed on IMF Multiplicity.

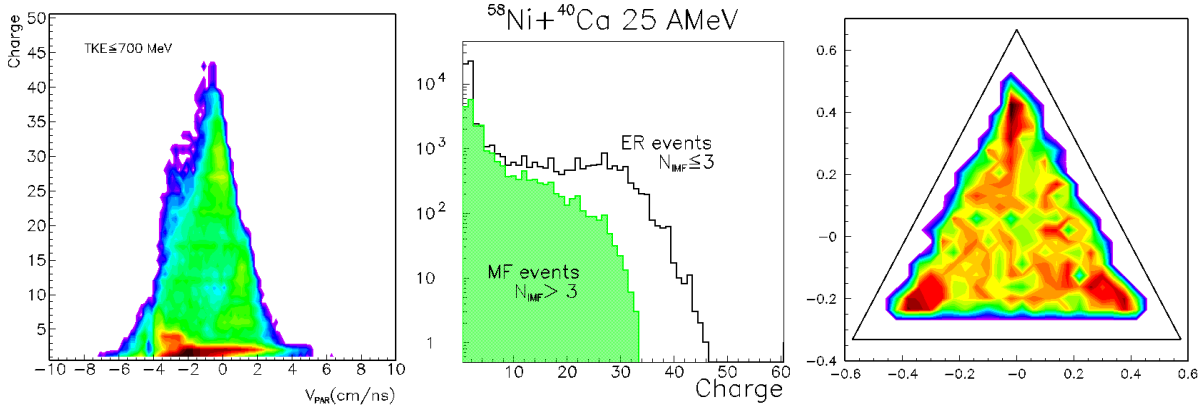

Fig.1: Charge of the produced fragments as a function of the parallel velocity to the beam direction in the CM reference frame (left panel) for central collisions; Charge distribution for the two subsets obtained imposing a further selection on IMF Multiplicity (middle panel); charge Dalitz plot for N_{IMF}>3 subset(right panel), where the coordinates for each event are assigned so that

$$x = \frac{1}{\sqrt{3}} \frac{Z_2 - Z_1}{\sum_{i=1}^{3} Z_i} \; and \; y = \frac{Z_3}{\sum_{i=1}^{3} Z_i} - \frac{1}{3}$$

In particular, events with N_{IMF}≤3 exhibited a charge distribution, shown in the middle panel of Fig.1, that recalls the U-shaped charge distribution characteristic of the low energy domain, while events with N_{IMF}>3 showed a monotonically decreasing charge distribution, typical of a multifragmentation phenomenon. In addition to the general trend of the charge distribution, information on the reaction mechanisms can be obtained by charge Dalitz plot, connected with the charge partition of the three biggest fragments. In the right panel of Fig.1 the Dalitz plot, obtained for events with N_{IMF}>3, is presented. It can be noted that the corners of the plot are highly populated, indicating that a big fragment is emitted together with two smaller ones. This distribution, usually observed for events where an evaporation residue is detected, is unexpected for a multifragmenting source, where the produced fragments are expected to be equally sized, thus populating the center of the triangle.

To understand if these events are to be ascribed to a multifragmenting source, which could have some peculiar behavior at these low excitation energies, or to a sequential decay of a composite system, a comparison of the experimental data with a semi-classical mean field theoretical model was performed.

2.3. Model Predictions

In order to identify the reaction mechanisms involved in the selected central collisions, comparisons with the predictions of a dynamical approach based on the Boltzmann-Langevin-One-Body (BLOB) model were conducted [8]. The BLOB approach describes clusterization as a result of large amplitude fluctuations acting in a semi-classical mean field framework, with the addition of a stochastic two-body collisional term. Differently from a first comparison performed in [9], where an impact parameter b=0 was used, results for simulations obtained imposing b=0-3 fm, for ^{58}Ni+^{40}Ca systems at 25 AMeV are shown hereafter. These impact parameter values were initially selected in order to have a more realistic reproduction of the experimental data; thereafter, it will be necessary to check the impact parameter values relative to the selected experimental subsample, using the Cavata method [11][12]. After a first stage of preequilibrium emission, which brings the composite system to N/Z value close to the stability

valley, a source of A=60-70 amu and atomic number Z=30, with an excitation energy of 2 AMeV, is expected.

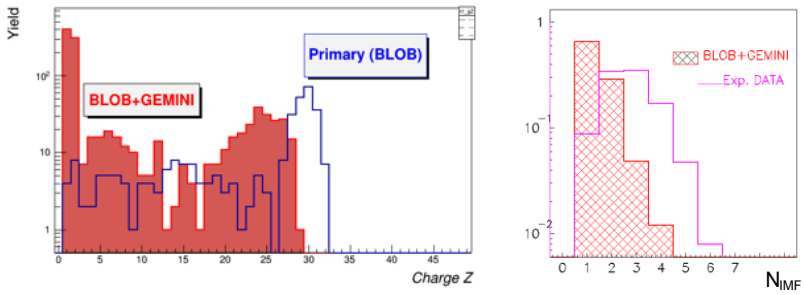

Fig.2: BLOB and GEMINI model predictions for ^{58}Ni+^{40}Ca system at 25 AMeV, for b =0-3 fm. Primary (blu line) and the final (red histogram) charge distributions (left panel); IMF multiplicity for BLOB+GEMINI simulations (red histogram) and for the experimental data (purple line)(right panel).

In the 18% of cases, the produced source (in around 300 fm/c) is composed by two primary fragments. The de-excitation of the primary source was simulated with GEMINI statistical sequential code [12]. The BLOB+GEMINI charge distribution (Fig.2, left panel) recalls the experimental Evaporation Residue type distribution. In addition, the BLOB+GEMINI IMF multiplicity distribution does not reproduce the tail at higher multiplicities exhibited by the experimental data, even if some events with 3 or 4 fragments in the final state are present (Fig.2, right panel). On the other hand, BLOB primary events with N_{IMF}=1 that would mimic the formation of a compound nucleus, after the secondary sequential decay simulated with GEMINI, present a number of IMF much lower than the number observed in the most dissipative events. In other words, a secondary sequential decay of a single fragment source would not produce events with $N_{IMF} \approx$ 4-6.
The comparison with BLOB simulations supports the idea that a Multifragmenting source is present, where fragments are formed simultaneously, even if the number of fragments estimated is lower than the experimental observed one. This can be caused by an underestimation of the excitation energy in BLOB or by some model parameters that need to be better tuned. From the experimental data point of view, in presence of a multifragmentation event, more symmetric charge fragment partitions are expected and a flat distribution of the cosine of flow angle, related to the topology of the events, namely to their shape in velocity space, should be observed. The absence of these behaviors is probably related to the fact that, at low incident energy and at moderate excitation energies, the persistence of a massive fragment is observed together with the productions of small IMFs, underlining the smooth transition from a fusion-evaporation reaction mechanism to a multifragmentation reaction mechanism. The comparison of results obtained for the systems at 25 AMeV incident energy with the 35AMeV results will shed some light on the reaction mechanisms involved. Additional simulations with CoMD (Constrained Molecular Dynamics) Model [13][14] are in progress.

3. ^{58}Ni+^{40}Ca at 35 AMeV

3.1. Experimental Data Detection

The second part of the experimental campaign was conducted, also at LNS, accelerating ^{58}Ni and ^{62}Ni beams at 35 AMeV on ^{40}Ca and ^{48}Ca targets. The same identification techniques of 25 AMeV runs were used, but the apparatus efficiency in the two experimental runs was a little different due to some geometrical modifications between the two experimental runs, performed about two years apart. Calibration of the raw data and identification of fragments with the different techniques are still in progress, thus only some preliminary results will be presented in the following.

3.2. Central Collisions Selection

A first attempt was made selecting the central collisions by means of cuts on TKE, as done for the lower incident energy. An inclusion of some semi-peripheral events was observed in the data subset, probably due to some discrepancies in the TOF calibration; thus it was decided to use as impact parameter selector the total charged multiplicity N_C, which does not involve variables related to the TOF-identification.

In Fig.3, left panel, the correlation of the charge as a function of the parallel velocity is presented for central collisions, selected imposing N_C>15. Fragment velocities show a broad distribution (probably due to the TOF calibration discrepancies) centered at CM velocity, indicating the emission of fragments formed in a single source. The maximum charge of fragments is around 20, confirming, at increasing incident energies, a decrease of mean field effects, which induces less nucleons to be bound in the transient composite system (source). The charge distribution, presented in the middle panel of Fig.3, shows a monotonical decrease, and the Dalitz plot (Fig.3, right panel) is now more populated in the center, supporting the idea that the fragments are more equally sized, coming from a multifragmenting source.

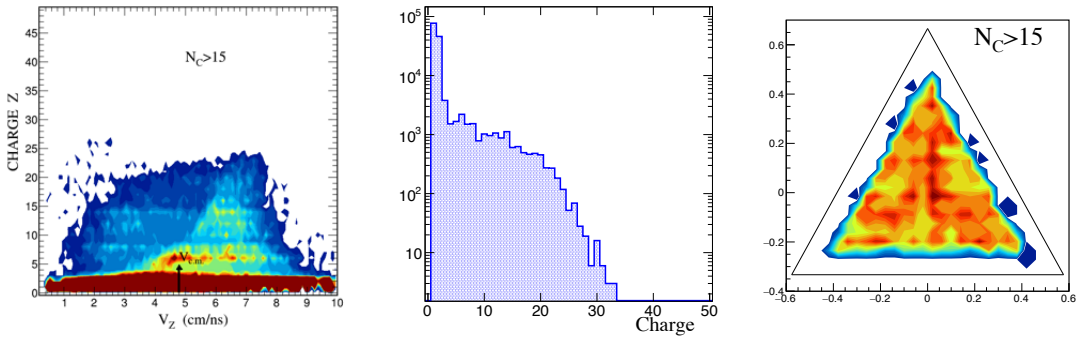

Fig.3: Preliminary results for central collisions at 35 AMeV, obtained imposing total charged Multiplicity N_C>15: charge of produced fragments as a function of the parallel velocity in the laboratory reference frame(left panel); charge distribution (middle panel); charge Dalitz plot (right panel)(see Fig.1 caption for axis label).

3.3. Model Predictions

Simulations were also performed for the ^{58}Ni+^{40}Ca system at 35 AMeV, for b=0-3 fm. A primary source with average values of A=60 amu and Z=27, with an excitation energy of 2 AMeV is predicted.

The sources, even with the same excitation energies as the 25 AMeV predictions, are now composed of 3 or 4 primary fragments, and the tail of IMF Multiplicity, obtained with BLOB+GEMINI, reaches values equal 5. Even if the predicted N_{IMF} is still not totally superimposed to the experimental one (right panel of Fig.4), the simulations well reproduce the number and the charge distribution of fragments. This supports the idea that, at this incident energy, the composite system formed in central collisions entered the spinodal region, characterized by a density value around one third of the saturation density, where volume instabilities amplify fluctuations, inducing clusterization.

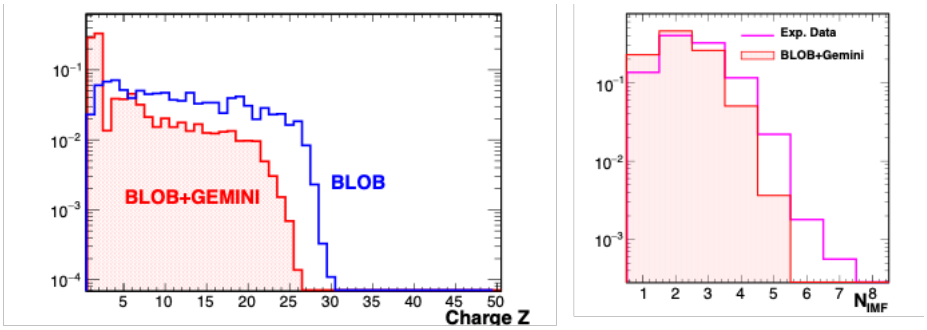

Fig4: Theoretical predictions of the charge distribution of primary and final fragments for b=0-3 fm reactions at 35 AMeV (left panel); experimental and theoretical IMF multiplicity (right panel).

4. Evolution of Fragment Production with Incident Energies

Even if the analysis of experimental data at 35 AMeV is not completed, some preliminary conclusions can be drawn. An evolution in the size of the produced fragments is observed for central collisions: low IMF multiplicity events can be associated to the formation of a massive fragment, which at 25 AMeV is reminiscent of the evaporation residue of the low energy domain, as, for example, supported by the U-shaped charge distribution (Fig.1, middle panel). However, the population of the corners of the Dalitz plot also for events at higher N_{IMF}, underlines a peculiar behavior that could be ascribed to the onset of multifragmentation: at lower incident energies the biggest fragment of the event, even in the most dissipative collisions, remains a very massive fragment. On the contrary, at higher incident energy, the charge distributions of the three biggest fragments (ordered in size) (Fig.5, middle panel) present lower dispersions, highlighting the typical features of fragments emitted in a multifragmentation process.

An evolution of the IMF multiplicity is also expected. At 35 AMeV a lower cross section for N_{IMF}=1,2 is expected with respect to the 25 AMeV one, and a higher probability of observing events with N_{IMF} =5-6 is predictable, differently from what is shown in the right panel of Fig.5. Even if the key parameter driving the number of fragments in a multifragmentation process is the excitation energy, and at this stage of the analysis we are not able to sort N_{IMF} as a function of excitation energies, it seems plausible that this effect is caused by the use of different impact parameter selectors. A selection of central collisions using the same variable of 25AMeV experimental data or variables related to the shape of the event in the tensor analysis will be performed as soon as the TOF calibration are verified. Moreover, Cavata method [11] will allow to verify the impact parameters selected for the central collisions at the two incident energies.

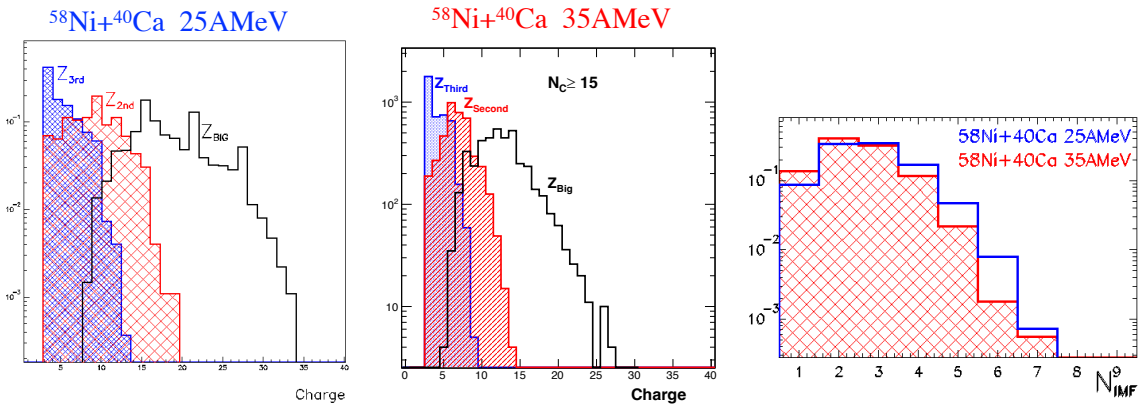

FIG.5: Charge distribution of the three biggest fragments at E_{beam}=25 AMeV (left panel) and E_{beam}=35 AMeV (middle panel); IMF Multiplicity N_{IMF} for central collisions in the two reactions (right panel).

5. Conclusions

The evolution of fragment production at the low range of Fermi energies, where the onset of Multifragmentation occurs, was analyzed for central collisions produced in ^{58}Ni+^{40}Ca at 25 and 35 AMeV. An evolution in the size of the produced fragments is observed, consisting in emitted fragment size decrease as the incident energy increases. A peculiar behavior that could be ascribed to the onset of multifragmentation is observed at lower incident energies where the biggest fragment of the event, even in the most dissipative collisions, remains a very massive fragment. Evolution in the IMF multiplicity will be studied as soon as excitation energies or impact parameters of the different reactions will be estimated.

The smooth appearance of multifragmentation phenomena, emphasizing the evolution of the reaction mechanisms, at the entering of the Fermi energies domain, allows to access regions of nuclear matter with a density ranging from the saturation values to lower ones, in order to investigate properties of the equation of state of nuclear matter far from stability [15][16][17][18].

References

[1] Durand D, Surand E and Tamain B 2001 *"Nuclear Dynamics in the nucleonic regime"* IOP
[2] Pirrone S et al 2019 *Eur. Phys. J A* ***55*** *22*
[3] Pirrone S et al 2014 *J. Phys. Conf. Ser.* **515** 012018
[4] Russotto P et al 2020 *Eur. Phys. J* A **56** 12
[5] Borderie B and Rivet MF 2008 *Progr. Part. Nucl. Phys* **61** 551–601
[6] D'Agostino M et al 2011 *Nucl. Phys.* A **861** 47–66
[7] Pagano A et al 2001 *Nucl. Phys. A* **681** 331
[8] Pagano A 2012 Nucl. *Phys. News* **22** 28 and references therein
[9] Geraci E et al 2020 *J. Phys.: Conf. Ser.* **1643** 012087
[10] Napolitani P and Colonna M 2013 *Phys. Lett B* **726** 382
[11] Cavata C et al 1990 *Phys. Rev. C* **42** 1760
[12] Charity R 2010 *Phys. Rev. C* **82** 014610
[13] Papa M et al 2015 *Phys. Rev. C* **91** 041601
[14] Papa M et al 2013 *Phys. Rev. C* **87** 014001
[15] Iglio J. et al 2006 *Phys. Rev. C* **74** 024605
[16] Russotto P, Cozma M, De Filippo E, Le Fèvre A, Leifels Y and Łukasik J 2023 *Riv. Nuovo Cimento* **46** 1-70
[17] Pagano A et al 2020 *Eur. Phys. J* A **56** 102
[18] Pagano A and De Filippo E 2014 *Eur Phys J* A **50** 32